

Correlations in intermediate-energy two-proton removal reactions

K. Wimmer,^{1,*} D. Bazin,¹ A. Gade,^{1,2} J. A. Tostevin,^{1,3} T. Baugher,^{1,2} Z. Chajecki,¹ D. Coupland,^{1,2} M. A. Famiano,⁴ T. K. Ghosh,⁵ G. F. Grinyer,^{1,†} R. Hodges,^{1,2} M. E. Howard,⁶ M. Kilburn,^{1,2} W. G. Lynch,^{1,2} B. Manning,⁶ K. Meierbachtol,^{1,7} P. Quarterman,^{1,2} A. Ratkiewicz,^{1,2} A. Sanetullaev,^{1,2} E. C. Simpson,³ S. R. Stroberg,^{1,2} M. B. Tsang,¹ D. Weisshaar,¹ J. Winkelbauer,^{1,2} R. Winkler,¹ and M. Youngs^{1,2}

¹*National Superconducting Cyclotron Laboratory, Michigan State University, East Lansing, Michigan 48824, USA*

²*Department of Physics and Astronomy, Michigan State University, East Lansing, Michigan 48824, USA*

³*Department of Physics, University of Surrey, Guildford, Surrey GU2 7XH, United Kingdom*

⁴*Department of Physics, Western Michigan University, Kalamazoo, Michigan 49008, USA*

⁵*Variable Energy Cyclotron Centre, 1/AF Bidhannagar, Kolkata 700064, India*

⁶*Department of Physics and Astronomy, Rutgers University, New Brunswick, New Jersey 08903, USA*

⁷*Department of Chemistry, Michigan State University, East Lansing, Michigan 48824, USA*

(Dated: October 10, 2018)

We report final-state-exclusive measurements of the light charged fragments in coincidence with ²⁶Ne residual nuclei following the direct two-proton removal from a neutron-rich ²⁸Mg secondary beam. A Dalitz-plot analysis and comparisons with simulations show that a majority of the triple-coincidence events with two protons display phase-space correlations consistent with the (two-body) kinematics of a spatially-correlated pair-removal mechanism. The fraction of such correlated events, 56(12) %, is consistent with the fraction of the calculated cross section, 64 %, arising from spin $S = 0$ two-proton configurations in the entrance-channel (shell-model) ²⁸Mg ground state wave function. This result promises access to an additional and more specific probe of the spin and spatial correlations of valence nucleon pairs in exotic nuclei produced as fast secondary beams.

PACS numbers: 24.10.-i 24.50.+g 25.60.Gc 29.38.-c

Access to nuclear reactions that can probe the states of pairs of nucleons in an atomic nucleus is a long-standing ambition. Specifically, an ability to probe the spin-structure of nucleon pairs and, for example, to identify and quantify two-nucleon correlations in the $[S, T]=[0, 1]$ spin-isospin channel, is required. Intermediate-energy reactions that remove two nucleons (2N) suddenly from a fast projectile, in collisions with a light target nucleus, have been shown [1–4] to provide a sensitivity to the 2N configurations near the projectile surface. Experimentally, the importance of nucleon removal reactions derives from their high detection efficiency (forward focusing of the reaction residues) and use of thick reaction targets, increasing the effective luminosity of the relatively low intensity exotic beams. Prior to the present work these 2N removal cross section measurements have been inclusive with respect to the final states of both the target and the removed nucleons but often exclusive with respect to the bound final-states of the forward-traveling projectile-like residues, allowing spectroscopic studies based on the different residue final-state yields and the shapes of their momentum distributions [5–10].

The present work sacrifices, temporarily, this better-understood residue final-state sensitivity to investigate new information that might be forthcoming from more exclusive measurements of the final states of the removed nucleons. The ⁹Be(²⁸Mg,²⁶Ne) reaction was used at an intermediate energy of 93 MeV/u. The chosen reaction was studied previously in a ²⁶Ne- γ coincidence measurement [10] and was used to confirm the predicted relative

populations of the four bound ²⁶Ne final states [1]. The present data set has also been used [11] to confirm that the measured contributions to the inclusive 2N-removal cross section from each of the possible elastic and inelastic removal mechanisms [1] were consistent with calculations that use eikonal reaction dynamics and sd -shell-model structure inputs for the ²⁸Mg to ²⁶Ne(J^π) 2p overlap functions. There it was shown that only 8(2) % of the inclusive ⁹Be(²⁸Mg,²⁶Ne) reaction cross section results from elastic breakup, the remainder being associated with reactions in which at least one of the removed protons interacts inelastically with the ⁹Be target nucleus [11].

The experiment was carried out at the Coupled Cyclotron Facility at the NSCL(MSU). The ²⁸Mg secondary beam was produced by projectile fragmentation of a 140 MeV/u ⁴⁰Ar primary beam and selected using the A1900 fragment separator [12]. The ⁹Be reaction target had a thickness of 100 mg/cm² and was placed at the target position of the high-resolution S800 magnetic spectrograph [13]. The beam energy at mid-target position was 93 MeV/u. The ²⁶Ne reaction residues were identified by measuring the energy loss in the ionization chamber in the S800 focal plane and the time of flight measured between scintillators before and after the reaction target. The ²⁶Ne energy and momenta were reconstructed from the measured positions and angles in the focal plane using the position-sensitive cathode readout drift chambers (CRDC) and ion optical ray-tracing. Protons and other light charged particles were detected and identified in the

high-resolution array HiRA [14]. Other experimental details and the angular coverage of HiRA were discussed in detail in Ref. [11]. In the present analysis we considered those triple-coincidence events where both of the light particles were identified as protons. These 4810 events represent 28(3) % of the inclusive two-proton removal cross section [11].

The continuum energy of these $^{26}\text{Ne}+p+p$ triple-coincidence events in their total momentum $P_{c12} = 0$ frame can be reconstructed from the three measured laboratory frame four-momenta P_i . Thus,

$$E_{\text{obs}} = \sqrt{(\sum P_i)^2} - \sum m_i \quad (1)$$

is the energy (above threshold) of the dissociated ^{28}Mg fragments, whose distribution is shown in Fig. 1(a). This distribution served as an input for Monte-Carlo kinematics simulations, used to populate the $^{26}\text{Ne}+p+p$ phase space and explore correlations of the detected protons.

In the simulations the three particles were assumed to be structure-less. There was no consideration of spin degrees of freedom of the two protons. Two kinematics scenarios were used, (a) three-body and (b) two-body, to generate the four-momenta of the three particles in the $P_{c12} = 0$ frame. The summed energies of the three particles were sampled from the experimental $d\sigma/dE_{\text{obs}}$ distribution shown in Fig. 1(a). In the three-body case the available energy E_{obs} was distributed among the three particles (democratic breakup). The residue and protons are then correlated only by energy and momentum conservation leading to the broad two-proton relative energy distribution shown in Fig. 1(b). The two-body case simulated events where the target was assumed to have encountered spatially-localized proton pairs (carrying energy ε^* in their $P_{12} = 0$ frame) and delivered an impulse to these pairs; as would be expected for some fraction of events in the 2N-removal reaction mechanism that favors the surface localization and spatial proximity of pairs of nucleons (see e.g. [4]). The energy E_{obs} was now shared between an assumed ε^* and the motion of the center-of-mass of the protons, producing $^{26}\text{Ne}+(2p)^*$ configurations that decay to $^{26}\text{Ne}+p+p$.

To study the two-proton correlations we first reconstruct the measured two-proton relative energy, E_{rel} , distribution shown in Fig. 1(b). These data points were fitted to extract the relative numbers of three-body (red) and two-body (green) kinematics events, the events for $E_{\text{rel}} > 40$ MeV being assumed to result from the three-body mechanism only. The fitted two-body events then determine the ε^* spectrum that is sampled to generate the two-body phase-space. We attribute the fraction 0.56(12) to these latter, correlated 2p-removal events. The two kinematics scenarios also show a different signature with respect to the angle between the protons. However, due to both the coarse and somewhat limited azimuthal angles coverage in the experiment, no addi-

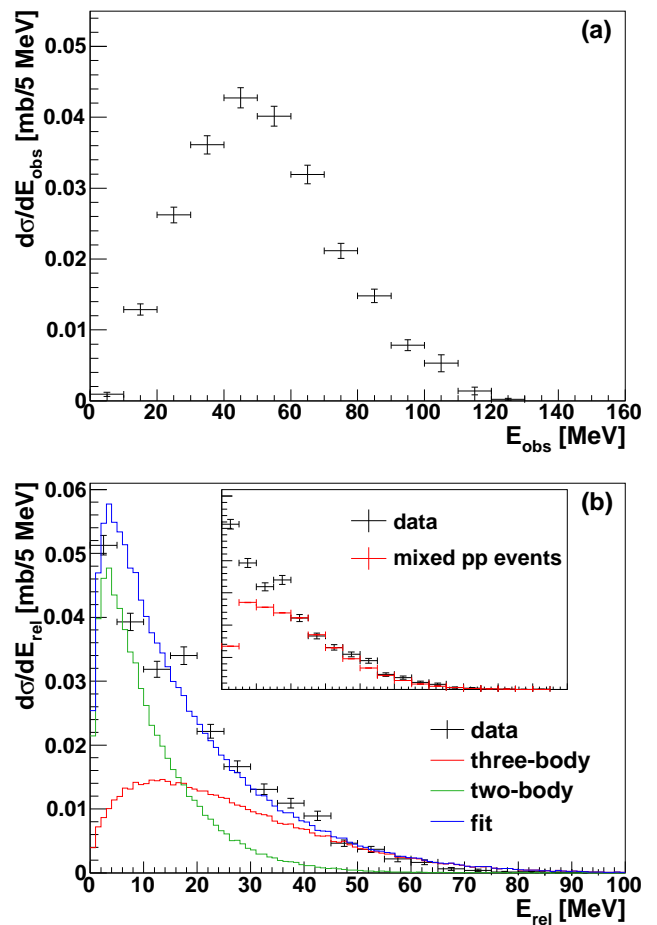


FIG. 1: (color online) (a) Energy of the dissociated $^{26}\text{Ne}+p+p$ fragments, in their $P_{c12} = 0$ frame. The cross section has been corrected for the geometric efficiency of the HiRA array, as described in [11]. (b) Relative energy distribution of the two detected protons. The fractions of simulated three-body (red) and two-body (green) kinematics events have been fitted to the data set (see text for details). The inset compares the measured relative energy distribution with that derived from mixing protons from two independent events (red). The distribution obtained from mixed events has been scaled to the experimental two-proton relative energy distribution above 40 MeV

tional useful evidence could be extracted from the measured angular distributions. We note that an E_{rel} distribution generated from mixed events – in which the two protons were completely uncorrelated – did not show the increase in the cross section for small E_{rel} , as is shown in the inset to Fig. 1(b).

Sequential two-proton removal events, via a single-proton removal to proton-unbound intermediate-states in ^{27}Na , are not considered to contribute. Such indirect paths would involve the proton decay of intermediate ^{27}Na excited states with energies in excess of 13.3 MeV, whereas the neutron threshold in ^{27}Na lies below 7 MeV in excitation energy [10]. This expectation is con-

firmed experimentally by the analysis of the Dalitz plot in Fig. 2, as will now be discussed.

In high-energy physics, three-particle final-states are commonly studied by the analysis of Dalitz plots [15]. This shows the correlation of the squares of the invariant masses $M_{ij}^2 = (P_i + P_j)^2$. In the absence of sources of two-particle correlations, the observed distributions will be uniform within the boundaries defined by energy and momentum conservation. Since the quantity on the Dalitz plot is proportional to the square of the matrix element for the system, intermediate states as well as symmetries generate a non-uniform distribution. In the present case, the boundaries will be different for each value of the continuum energy, E_{obs} , so we have adopted the approach of Ref. [16] and used the normalized invariant masses, W_{ij} , that range from 0 to 1, i.e.

$$W_{ij}^2 = \frac{M_{ij}^2 - (m_i + m_j)^2}{(E_{\text{obs}} + m_i + m_j)^2 - (m_i + m_j)^2}. \quad (2)$$

The Dalitz plot of the current $^{26}\text{Ne}+p+p$ event data is shown in Fig. 2(a). The experimental results are compared to the three-body and two-body 2p-removal kinematics simulations using a two-body fraction of 0.56 in panel (d). The three-body case results in a flat distribution while the two-body kinematics simulation produces a non-uniform filling of the phase space – with an increased intensity at lower proton-proton invariant masses W_{pp} .

If present, sequential two-proton removal via an excited intermediate state in ^{27}Na would lead to vertical bands with constant W_{cp}^2 , as is shown in panel (e). This was not observed in the experimental data, providing strong support for our assumption that such indirect paths do not contribute. This provides a direct experimental confirmation of earlier arguments, based on energetics, the cross section, and the inclusive momentum distribution, for the dominance of the direct removal of the two strongly-bound valence particles [1, 10].

Also shown, in panels (b) and (c) of Fig. 2, are the data projections onto the W_{pp}^2 and W_{cp}^2 axes. These data projections are also reasonably well described by the combination of the two breakup modes determined from the fit to the relative energy spectrum, Fig. 1(b). We note that the effect of the ^9Be reaction target enters the simulations only very indirectly, through the measured projectile excitation energy distribution, $d\sigma/dE_{\text{obs}}$ of Fig. 1(a). Thus, the comparisons of the data with the two simulated kinematics scenarios does not provide information on the final states of the target, to which our results remain inclusive.

It is instructive to compare the deduced correlated 2p-fraction to the calculated two-nucleon spin contributions to the reaction cross sections. The partial cross sections to each $^{26}\text{Ne}(J^\pi)$ final state receive incoherent (additive) contributions from the total orbital L and spin S angular momentum components in the $(^{26}\text{Ne}(J^\pi)|^{28}\text{Mg})$ two-proton overlaps [2]. Table I shows the $S=0$ fractions (%)

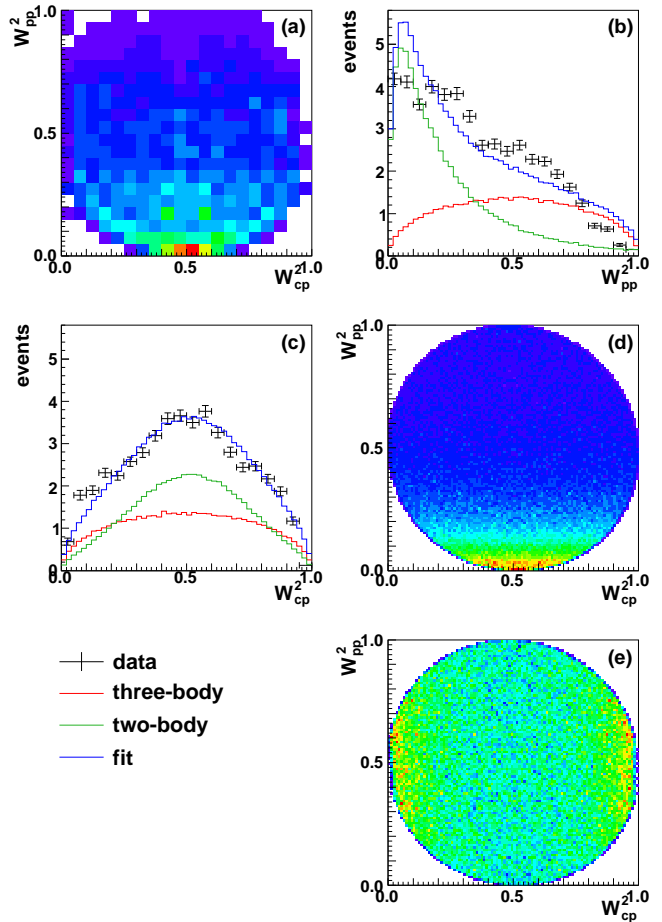


FIG. 2: (color online) Dalitz plots of core (^{26}Ne residue)-proton W_{cp} and proton-proton W_{pp} invariant masses. Panel (a) shows the experimental data with projections on W_{pp}^2 (b) and W_{cp}^2 (c). The results of the simulation using a two-body fraction of 0.56 are shown in panel (d). Panel (e) shows the corresponding Dalitz plot for simulated sequential two-proton removal events, via a single-proton removal to a proton-unbound intermediate-state in ^{27}Na .

of both the overlaps and the removal cross sections, $\sigma_{S=0}$, when using the sd -shell-model two-nucleon amplitudes tabulated in Ref. [17]. These $[S, T]=[0, 1]$ wave function components will have significant but not exclusively 1s_0 2p configurations.

The relative transparency of the direct reaction mechanism to the S of the two nucleons delivered by the projectile is evident from Table I. The $S = 0$ fractions of the overlaps are reflected rather directly, with only small final-state-dependent enhancements, in their percentage contributions to the cross sections, $\sigma_{S=0}$. Here the $S=0$ terms are seen to be responsible for 64 % of the computed inclusive cross section, consistent with the two-body event fraction deduced from the simulations. This suggests that the $[S, T]=[0, 1]$ correlations present in that part of the ^{28}Mg ground-state wave function sampled by

TABLE I: Calculated partial and inclusive cross sections for the $^{28}\text{Mg}(-2p)$ reaction at 93 MeV per nucleon and the percentage contributions of $S=0$ terms to the two-proton overlaps and the cross sections. The 2p stripping contributions are shown in Table III of Ref. [17], there for 82.3MeV/nucleon.

J_f^π	E (MeV)	Overlap ($S=0$, %)	σ_{th} (mb)	$\sigma_{S=0}$ (mb)	$\sigma_{S=0}$ (%)
0^+	0.0	86	1.190	1.083	90
2^+	2.02	18	0.327	0.071	22
4^+	3.50	38	1.046	0.523	49
2_2^+	3.70	50	0.458	0.250	54
Incl.			3.02	1.93	64

the target may be maintained in the sudden two-proton removal process and be reflected, here via the two-body kinematics events simulation, as two-proton correlations in the final state.

This being the case, an expectation is that the width of the parallel momentum distribution of residues, gated on the two-body-like events with smaller E_{rel} , should be narrower; this due to the size of the $^{26}\text{Ne}(0^+)$ ground state cross section with its narrow momentum distribution [3]. However, as all ^{26}Ne final states contribute significantly to the 64 % $S=0$ contribution to the inclusive cross section, this differential width is only slightly larger than our current experimental resolution. Fig. 3 shows the parallel momentum distribution of the ^{26}Ne residues (in coincidence with two protons) gated on two-body and three-body events. We only consider the central part of momentum distributions since the high and low-momentum tails were influenced by acceptance cut-offs and proton detection thresholds. The parallel momentum distribution gated on three-body mechanism events (red line in Fig. 3) is slightly wider than the corresponding distribution gated on two-body events. This differential width effect is consistent with what is expected based on the theoretical $S=0$ and $S=1$ momentum distributions folded with the width of the momentum distribution of the unreacted ^{28}Mg beam. Since the two- and three-body simulations describe the available data, and the extracted momentum distributions are consistent, within statistics, with the two-body events being closely allied with the $S=0$ overlap function components, we may expect that the less-spatially-localized $S=1$ two-proton components will track the results of the three-body simulation. Additional data, e.g. to states with different $S=0, 1$ fractions will be needed to confirm this expectation.

In summary, we have observed significant kinematical correlations of two final-state protons measured in coincidence with ^{26}Ne residues following the $^9\text{Be}(^{28}\text{Mg}, ^{26}\text{Ne})$ two-proton removal reaction. We attribute the deduced 56(12) % fraction of two-body events to the observed cross section as due to spin $S=0$ two-proton configurations in the ^{28}Mg wave function in the entrance-channel. This result suggests the potential for such measurements

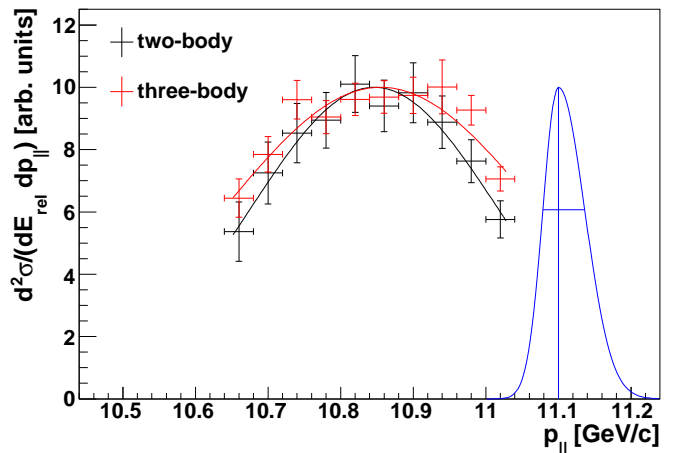


FIG. 3: (color online) Parallel momentum distribution of the ^{26}Ne residue gated on two-body (black) and three-body (red) events. The two components were extracted by applying a cut on E_{rel} at the intersection of the two distributions in Fig. 1(b). Contributions from three-body events at low E_{rel} were subtracted from the two-body distribution and vice-versa for the two-body events with high relative energy. The lines are Gaussian fits. The two distributions have been normalized to show the difference in width. The blue distribution illustrates the width of the momentum distribution of the incoming ^{28}Mg beam.

to provide an additional, more specific probe of the spin correlations of valence nucleon pairs in exotic nuclei. It also suggests the need for additional exclusive measurements to confirm and quantify this proposed spin sensitivity. Specifically, two-nucleon removal reactions to nuclei with only a single (0^+) bound state, where $S=0$ configurations will dominate, would be ideally suited for this kind of study. Further indirect indications of $S=0$ driven final-state 2p correlations could come from observations of enhanced ^3He and α -particle yields produced following 1n- or 2n-pickup from the target by $S=0$ 2p configurations in their surface-grazing removal collisions.

This work was supported by the National Science Foundation under Grants Nos. PHY-0606007, PHY-0757678 and PHY-1102511, and the UK Science and Technology Facilities Council (STFC) under Grant No. ST/J000051/1.

* Present address Central Michigan University, Mt. Pleasant, Michigan 48859, USA

† Present address GANIL, CEA/DSM-CNRS/IN2P3, Bvd Henri Becquerel, 14076 Caen, France

- [1] J. A. Tostevin and B. A. Brown, Phys. Rev. C **74**, 064604 (2006).
- [2] E. C. Simpson and J. A. Tostevin, Phys. Rev. C **82**, 044616 (2010).
- [3] E. C. Simpson, J. A. Tostevin, D. Bazin, B. A. Brown, and A. Gade, Phys. Rev. Lett. **102**, 132502 (2009).

- [4] E. C. Simpson, J. A. Tostevin, D. Bazin, and A. Gade, *Phys. Rev. C* **79**, 064621 (2009).
- [5] K. Yoneda et al., *Phys. Rev. C* **74**, 021303 (2006).
- [6] J. Fridmann et al., *Phys. Rev. C* **74**, 034313 (2006).
- [7] B. Bastin et al., *Phys. Rev. Lett.* **99**, 022503 (2007).
- [8] P. Fallon et al., *Phys. Rev. C* **81**, 041302 (2010).
- [9] D. Santiago-Gonzalez et al., *Phys. Rev. C* **83**, 061305 (2011).
- [10] D. Bazin, B. A. Brown, C. M. Campbell, et al., *Phys. Rev. Lett.* **91**, 012501 (2003).
- [11] K. Wimmer, D. Bazin, A. Gade, J. A. Tostevin, et al., *Phys. Rev. C* **85**, 051603 (2012).
- [12] D. J. Morrissey, B. M. Sherrill, M. Steiner, A. Stolz, and I. Wiedenhoever, *Nucl. Instrum. Methods Phys. Res. B* **204**, 90 (2003).
- [13] D. Bazin, J. A. Caggiano, B. M. Sherrill, J. Yurkon, and A. Zeller, *Nucl. Instrum. Methods Phys. Res. B* **204**, 629 (2003).
- [14] M. S. Wallace, M. A. Famiano, M.-J. van Goethem, et al., *Nucl. Instrum. Methods Phys. Res. A* **583**, 302 (2007).
- [15] R. H. Dalitz, *Phys. Rev.* **94**, 1046 (1954).
- [16] F. M. Marqués, M. Labiche, N. A. Orr, et al., *Phys. Rev. C* **64**, 061301 (2001).
- [17] J. A. Tostevin, G. Podolyák, B. A. Brown, and P. G. Hansen, *Phys. Rev. C* **70**, 064602 (2004).